Molecular Vision 2017; 23:39-51 <http://www.molvis.org/molvis/v23/39>
Received 30 October 2016 | Accepted 23 February 2017 | Published 26 February 2017

© 2017 Molecular Vision

EBM regeneration and changes in EBM component mRNA expression in stromal cells after corneal injury

Abirami Santhanam,[1] Gustavo K. Marino,[1,2] Andre A. M. Torricelli,[1,2] Steven E. Wilson[1]

[1]Cole Eye Institute, Cleveland Clinic, Cleveland, OH; [2]University of Sao Paulo, Sao Paulo, Brazil

Purpose: To investigate the production of the epithelial basement membrane (EBM) component mRNAs at time points before lamina lucida and lamina densa regeneration in anterior stromal cells after corneal injury that would heal with and without fibrosis.

Methods: Rabbit corneas were removed from 2 to 19 days after −4.5D or −9.0D photorefractive keratectomy (PRK) with the VISX S4 IR laser. Corneas were evaluated with transmission electron microscopy (TEM) for full regeneration of the lamina lucida and the lamina densa. Laser capture microdissection (LCM) based quantitative real-time (RT)–PCR was used to quantitate the expression of mRNAs for laminin α-3 (LAMA3), perlecan, nidogen-1, and nidogen-2 in the anterior stroma.

Results: After −4.5D PRK, EBM was found to be fully regenerated at 8 to 10 days after surgery. At 4 days after PRK, the nidogen-2 and LAMA3 mRNAs levels were detected at statistically significantly lower levels in the anterior stroma of the −9.0D PRK corneas (where the EBM would not fully regenerate) compared to the −4.5D PRK corneas (where the EBM was destined to fully regenerate). At 7 days after PRK, nidogen-2 and LAMA3 mRNAs continued to be statistically significantly lower in the anterior stroma of the −9.0D PRK corneas compared to their expression in the anterior stroma of the −4.5D PRK corneas.

Conclusions: Key EBM components LAMA3 and nidogen-2 mRNAs are expressed at higher levels in the anterior stroma during EBM regeneration in the −4.5D PRK corneas where the EBM is destined to fully regenerate and no haze developed compared to the −9.0D PRK corneas where the EBM will not fully regenerate and myofibroblast-related stromal fibrosis (haze) will develop.

Defective regeneration of the corneal epithelial basement membrane (EBM) has been shown to be a critical factor in the development of stromal myofibroblasts and the development of stromal fibrosis (opacity or haze) after injury, surgery, or infection of the cornea [1-4]. Studies suggest that the normal EBM modulates the penetration of epithelium-derived growth factors, including transforming growth factor β (TGFβ) and platelet-derived growth factor (PDGF), that drive the development and persistence of myofibroblasts [5,6] from keratocyte- and bone marrow–derived precursor cells [3,4,7,8]. Studies in the cornea [9-11] and other organs [12-19] have demonstrated that fibroblastic or mesenchymal cells produce basement membrane components and likely contribute to the development and regeneration of the basement membrane associated with normal tissue morphology and function.

Using transmission electron microscopy (TEM), the ultrastructure of the normal EBM includes the lamina lucida and the lamina densa (Figure 1C). Although the actual appearance of the lamina lucida and the lamina densa noted with TEM may be an artifact of fixation [20], their presence in tissues fixed for traditional TEM is an indicator of normal structural composition in vivo [20]. Photorefractive keratectomy (PRK) in rabbit corneas provides a well-characterized and reproducible model for normal and defective EBM regeneration. Corneas that have low-correction PRK (−4.5D, for example) have normal regeneration of EBM over approximately 1 to 2 weeks (Figure 1C) and remain relatively transparent without the development of stromal myofibroblasts, whereas corneas that have high-correction PRK (−9.0D, for example) have abnormal regeneration of EBM (Figure 1D) without the regeneration of the lamina lucida and the lamina densa and acquire stromal fibrosis (haze or opacity) associated with the development and persistence of mature myofibroblasts in the stroma [1,4]. These same correlations between the level of PRK correction and the healing of the cornea with or without anterior stromal fibrosis are also noted in human corneas that are not treated with mitomycin C except that the proportion of human corneas that develop haze after high-correction PRK is much lower (2% to 5%) [21,22] than it is in the rabbit (100%) [1], and the time course for the development of maximal fibrosis is much longer in humans (approximately 3 to 4 months) [21,22] than it is in the rabbit (approximately 1 month) [1].

Correspondence to: Steven E. Wilson, Cole Eye Institute, I-32, Cleveland Clinic, 9500 Euclid Ave, Cleveland, Oh 44195; Phone: (216) 444 5887; FAX: (216) 445 8475; email: wilsons4@ccf.org

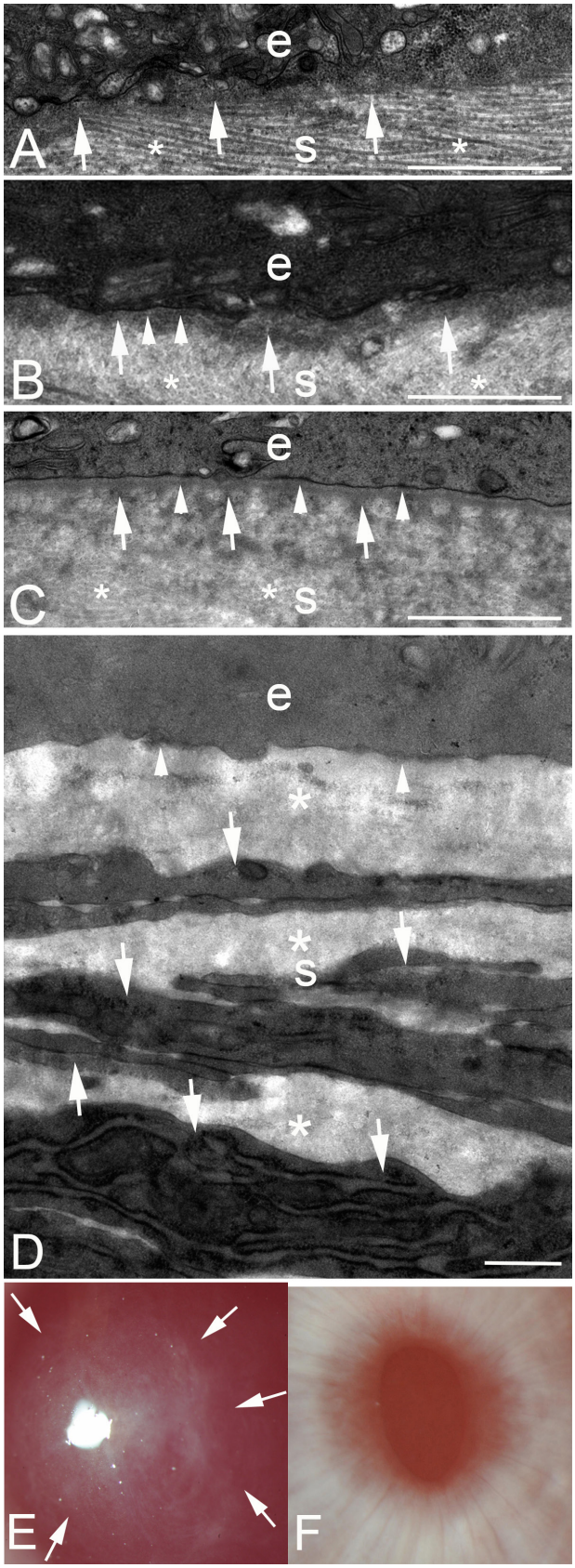

Figure 1. Transmission electron microscopy of the junction between the epithelium and the stroma at different time points after low-correction −4.5D photorefractive keratectomy (PRK) or high-correction −9.0D PRK in rabbits. e, epithelium; s, stroma. **A**: In a cornea at 7 days after −4.5D PRK, no discernable lamina lucida or lamina densa is present. Note, by chance, the specimen was cut such that the stacked collagen lamellas (*) are seen in the stroma. Dense deposits of extracellular matrix (arrows) can be seen in the stroma just posterior to the epithelium. Magnification = 23,000X. **B**: In a cornea at 8 days after −4.5D PRK, most of the excimer laser-ablated zone had no lamina lucida or lamina densa. However, in one area (arrowheads) nascent lamina lucida and lamina densa can be noted. Again, dense extracellular matrix seen in the stroma just posterior to the epithelium. In the stroma, collagen lamellas (*) that have been cut transversely can be noted. Magnification = 23,000X. **C**: In a cornea at 9 days after −4.5D PRK, there is a complete lamina lucida and lamina densa (arrowheads) across 100% of the excimer laser-ablated zone. Again, the dense extracellular matrix is noted just posterior to the intact epithelial basement membrane (EBM). In the stroma, collagen lamellas (*) that have been cut transversely can be noted. **D**: In a cornea at 1 month after −9.0D PRK that developed severe stromal fibrosis (haze), no normal EBM is detected beneath the epithelium (arrowheads). The anterior stroma is filled with stacked myofibroblasts (arrows) with large amounts of intracellular rough endoplasmic reticulum and surrounding disorganized extracellular matrix (*) that are the alpha-smooth muscle action+ (α-SMA) cells noted in Figure 2A. Magnification = 23,000X. **E**: Slit-lamp photograph of a rabbit cornea at 1 month after −9.0D PRK. Note the dense haze (arrows) in the central excimer laser-treated cornea with the pupil dilated. Magnification = 40X. **F**: Slit-lamp photograph of a rabbit cornea at 1 month after −4.5D PRK. Note the cornea is clear without fibrosis, and thus, the iris details are clear. Magnification = 40X. Scale bars (**A**–**D**) = 2 µm.

The corneal EBM is assembled from four primary components: collagens (including collagen type IV), laminins (including laminin 332), heparan sulfate proteoglycans (HSPGs; including perlecan, Hspg2), and nidogens (1 and 2) [23-26]. Many other components, such as fibronectin, are also present, and some components are tissue specific [23-26]. The lamina lucida and the lamina densa layers that are present in the normal corneal EBM but absent in corneas with fibrosis [1] are composed of specific components that include perlecan, nidogen-1 and -2, and laminin 332 [26].

In the current study, TEM was used to study the time to full regeneration of the EBM lamina lucida and lamina densa after low correction −4.5D PRK in rabbits. This timing knowledge was then applied to use laser capture microdissection (LCM) [27,28] to study the expression of mRNAs coding for nidogen-1, nidogen-2, perlecan, and laminin α-3 (LAMA3) in the anterior stroma of rabbit corneas at time points before the anticipated appearance of the fully regenerated lamina lucida and lamina densa after PRK to evaluate potential differences in the stromal expression of these key EBM components in corneas destined to heal with normal transparency (after low correction, −4.5D PRK) and corneas destined to heal with fibrosis (after high correction, −9.0D).

METHODS

Animals and PRK surgery: The Animal Control Committee at the Cleveland Clinic Foundation approved all animal studies described in this work. All animals were treated in accordance with the tenets of the ARVO Statement for the Use of Animals in Ophthalmic and Vision Research. Anesthesia was obtained by intramuscular injection of ketamine hydrochloride (30 mg/kg) and xylazine hydrochloride (5 mg/kg). In addition, topical proparacaine hydrochloride 1% (Alcon, Ft. Worth, TX) was applied to each eye just before surgery. Euthanasia was performed using an intravenous injection of 100 mg/kg pentobarbital while the animal was under general anesthesia.

Female New Zealand white rabbits, 12- to 15-weeks-old, weighing 2.5 to 3.0 kg each, were included in this study. One eye of each rabbit was selected at random for PRK surgery. Contralateral eyes were used in the control groups since no contralateral fibrosis effects have been detected after PRK. PRK with a 6.0 mm ablation zone was performed under general and topical anesthesia by placing an eyelid speculum within the interpalpebral fissure and removing 7 mm of the central corneal epithelium with a #64 Beaver blade (Becton-Dickinson, Franklin Lake, NJ) and using a VISX Star S4 IR excimer laser (Abbott Medical Optics, Irvine, CA) to apply either −4.5D or −9.0D spherical ablation to the anterior stroma overlying the pupil. One drop of Vigamox (Alcon) was applied to the PRK and control cornea four times a day until the epithelium healed. The epithelium healed within 3 to 5 days in all corneas, and there was no statistically significant difference in the time to epithelial closure between the −4.5D and −9.0D groups.

Immunocytochemistry for alpha-smooth muscle actin: At different time points after PRK, the rabbits were euthanized, and the corneoscleral rims of the treated and untreated contralateral eyes were removed without manipulation of the cornea using 0.12 mm forceps and sharp Westcott scissors. For immunohistochemical analyses, the corneas were immediately embedded in liquid optimal cutting temperature (OCT) compound (Sakura FineTek, Torrance, CA). The corneas were centered within the mold so that the block could be bisected, and transverse sections cut from the center of the cornea. The frozen tissue blocks were stored at −80 °C until sectioning was performed. Central corneal sections (7 µm thick) were cut with a cryostat (HM 505M, Micron GmbH, Walldorf, Germany). Sections were placed on 25 mm × 75 mm × 1 mm microscope slides (Superfrost Plus, Fisher) and maintained frozen at −80 °C until staining was performed [8].

Immunohistochemistry was performed as previously described [1] to identify myofibroblast cells in the stroma. Immunofluorescent staining for alpha-smooth muscle actin (α-SMA) was performed using a mouse monoclonal anti-human alpha-smooth muscle actin clone 1A4 (Dako, Carpinteria, CA). The sections were viewed and photographed with a Leica DM5000 microscope equipped with Q-imaging Retiga 4000RV (Surrey, BC, Canada) camera and ImagePro software (Leica Microsystems, Buffalo Grove, IL).

Transmission electron microscopy: TEM samples were prepared using the methods described by Fantes et al. [29]. Briefly, corneas at different time points after PRK or the control corneas were immediately placed in 2.5% glutaraldehyde and 4% paraformaldehyde with 0.2 M cacodylate buffer immediately after removal of the cornea and the scleral rim, and then the specimens were left in the fixative for a minimum of 24 h. The corneas were then rinsed with 0.2 M cacodylate buffer three times for 5 min each, post-fixed in 1% osmium tetroxide for 60 min at 4 °C, and dehydrated in increasing concentrations of ethanol from 30% to 95% for 5 min each at 4 °C. Finally, dehydration was performed using three 10 min rinses in 100% ethanol at room temperature and three 15 min rinses with propylene oxide at room temperature. Excised blocks of central anterior cornea were then embedded in epoxy resin medium. One micrometer thick sections cut perpendicular to the anterior corneal surface were stained with toluidine blue for orientation and light microscopy.

Ultrathin 85 nm thick sections were cut with a diamond knife, stained with 5% uranyl acetate and lead citrate, and observed using a Phillips CM12 transmission electron microscope operated at 60 kV (FEI Company, Hillsboro, OR).

Laser capture microdissection: The corneal tissues were fixed in the same way as described for immunocytochemistry in OCT compound and were immediately flash frozen using 2-methyl-butane in liquid nitrogen. Cryosections were cut from the central cornea with a Leica CM 1850 cryostat (Leica Microsystems Ltd., Milton Keynes, UK) with tissue thickness ranging between 12 and 15 µm. Collection and processing of the tissue, including RNA extraction, were performed under RNase free conditions. Immediately before LMD, cryosections on polyethylene terephthalate (PET) membrane slides (MicroDissect GmbH, Herborn, Germany) were stained with Arcturus Histogene staining solution (Thermo Fisher Scientific, Columbus, OH; Figure 2). Laser capture microdissection was performed using a Leica AS LMD system (Leica Microsystems, Wetzkar, Germany). The laser parameters, such as the focal diameter of the beam, magnification, and numerical aperture of the applied objective lens, were adjusted for optimal results. LCM sections of thickness 35 µm (area about 40,000 μm^2) were cut from the anterior stroma (AS) beneath the EBM of each cornea. The sections were collected in 0.5 ml tubes containing 70 µl of RNA*later* RNA Stabilization Reagent (Ambion).

Histological identification and isolation of anterior stromal cells from the cornea: To accurately dissect the AS from corneal sections, it was important to localize the corneal layers. Arcturus Histogene (Applied Biosystems, Roseland, NJ) staining allowed visualization of the epithelium, EBM, and stroma during laser microdissection (Figure 2). Since rabbit corneas do not have a Bowman's layer, the region immediately posterior to the EBM was laser outlined such that the LCM specimen was 36 µm thick and limited to the central 6 mm of cornea that had been ablated during PRK or stromal tissue of similar thickness and position in control corneas that did not have PRK. The thickness of the AS specimens laser dissected from all corneas (after PRK and unwounded controls) was determined in a pilot experiment with nine corneas at 1 month after haze-producing −9.0D PRK that had immunohistochemistry for α-SMA and the average thickness of the α-SMA+ layer beneath the EBM in the excimer laser-ablated central cornea was found to be a minimum of 36 µm thick beneath the EBM (Figure 2).

Extraction of total RNA and synthesis of cDNA: RNA was isolated from corneal tissue specimens cut from each individual PRK or unwounded control cornea obtained with LCM using RNeasy micro kit solution (Qiagen, Valencia, CA), and the total RNA was extracted, according to the manufacturer's instructions. The cDNA for each cornea was synthesized from total RNA (75 ng) with the Thermoscript RT–PCR System (Thermo Fisher Scientific) using oligo (dT) primers according to the manufacturer's instructions.

Quantitative real-time PCR: Initial screening of cDNA for different genes of interest was performed using real-time PCR (RT–PCR). Primers were designed using Primer3 combined with BLAST from NCBI (Bethesda, MD) and primers (Table 1) were synthesized by Integrated DNA Technologies (Coralville, IO).

The quantitative measurement of nidogen-1, nidogen-2, perlecan, and LAMA3 mRNA levels from different corneal layers was performed with real-time PCR using a DNA Engine Opticon system (MJ Research, MA) with the SYBR Green PCR Master Mix (BioRad) in a one-step reaction according to the manufacturer's instructions. The thermal cycle was programmed for 30 s at 98 °C for initial denaturation, followed by 35 cycles of 10 s at 98 °C for denaturation, 10 s at 59°C for annealing, 10 s at 72 °C for extension, and 1 min at 72 °C for the final extension. The melting curves and gel electrophoresis of the end products were obtained to confirm the specificities of the PCR reactions. The relative quantification of target genes was determined using the $\Delta\Delta^{Ct}$ quantitative RT–PCR method [30].

Statistical analysis: A sample size of four corneas (four corneas from different animals) was used for each −4.5D, −9.0D, and normal unwounded control group at each time point in all experiments. Each experiment was repeated at least once. All data are represented as the mean ± standard deviation (SD), and the statistical significance of the difference among the −4.5D PRK corneas, −9.0D PRK corneas, and unwounded control corneas at each time point was analyzed using a non-parametric Kruskal–Wallis test. A p value of less than 0.05 was considered statistically significant.

RESULTS

Time to full regeneration of the lamina lucida and the lamina densa after −4.5D PRK: Table 2 shows the results from 14 corneas of different rabbits that were analyzed with TEM at 23,000X to determine if there was full regeneration of the lamina lucida and the lamina densa over 100% of the excimer laser-ablated zone at time points from 7 to 19 days after surgery. Full regeneration of the EBM ultrastructure occurred between 8 and 10 days following −4.5D PRK. Figure 1 shows the TEM of representative corneas after −4.5D PRK. In Figure 1A, a cornea at 7 days after PRK had no evidence of the lamina lucida or the lamina densa throughout the excimer laser-ablated zone. In Figure 1B, a cornea at 8 days after PRK

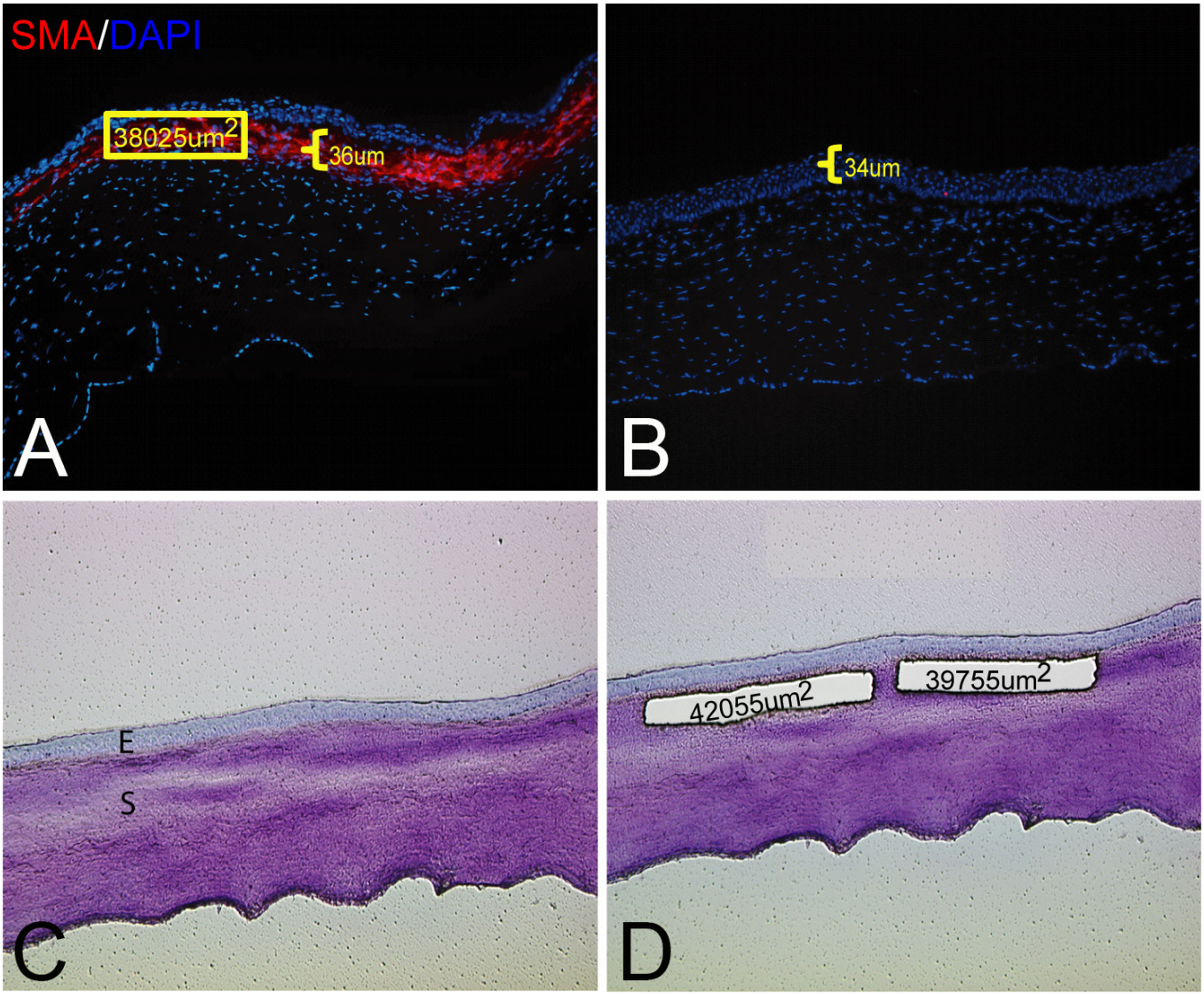

Figure 2. LCM strategy. **A**: Representative cornea stained for alpha-smooth muscle actin (α-SMA) and 4',6-diamidino-2-phenylindole (DAPI) at 1 month after −9.0D PRK. The indicated α-SMA+ myofibroblast layer was 36 µm thick according to the ImagePro software. This was the minimum thickness measured in nine pilot corneas at 1 month after −9.0D photorefractive keratectomy (PRK). The nuclei of all cells were stained with DAPI. **B**: Representative cornea stained for α-SMA at 1 month after −4.5D PRK. Note that no α-SMA+ myofibroblasts were detected in the stroma. The epithelium was 34 µm thick. **C**: Corneal section stained with Arcturus Histogene before laser capture microdissection (LCM). E, epithelium; S, stroma. **D**: The same corneal section after removal of two 36 µm thick specimens from the stroma immediately posterior to the epithelial basement membrane (EBM). The areas of the two cut specimens that dropped from the laser-cut polyethylene terephthalate (PET) membrane slide directly into a microtube with 70 µl of RNA*later* RNA stabilization reagent (Ambion) is shown. Magnification = 400X.

for the most part had no ultrastructural regeneration of the lamina lucida or the lamina densa, but there were small areas where nascent lamina lucida and lamina densa regeneration was detected. In Figure 1C, a cornea at 9 days after PRK had full ultrastructural regeneration of the lamina lucida and the lamina densa throughout the excimer laser-ablated zone. A small stretch of that zone is shown in the high magnification TEM image (Figure 1D). Note at all time points shown there were cells in the anterior corneal stroma immediately beneath the epithelium or the EBM. A slit-lamp photograph of a rabbit cornea at 1 month after −9.0D PRK shows dense haze in the central cornea, whereas in −4.5D PRK the cornea is clear without fibrosis, and thus, the iris details are clear (Figure 1E,F).

Table 1. PCR primers designed for LCM-RT–PCR.

Gene	Primer sequences (5'-3')	Size (bp)	Annealing (°C)	GenBank accession
NID1	F: ATGGGTTCAGCATCACTGGG R: TAATGACCAGCTTGCCTGGG	81	58	XM_017347600.1
NID2	F: CGTGCAAGACACGGAAGTCA R: GAGTTGGCTGGGACGTAAGG	141	58	XM_008269653.2
HSPG2	F: CGTGGCAGTCAACACCAAAG R: TTCTTGATGCAGCCCGTGAT	105	58	XM_017346486.1
LAMA3	F: CTCCCAAATGCCTCGTTCCT R: TTTGTACCGCACCCTGAGAC	138	58	XM_002713604.1
KERA	F: AGTGCGGATGACTTTGATTG R: TGGCTTCTCTGGAATGGTTT	165	58	XM_002711384.3
KRT12	F: GGCTCTCTGTATCTCCCCTCT R: CCATTTCCACGCTGACCT	541	59	XM_002719366.3
KRT3	F: ATGTCCGTGGTGCTGTCC R: GCTGGCGTTCTGCTTCTT	267	60	XM_002711005.2
ACTB	F: CACCCTCTCTCGACGAAACC R: CTGTCACCTTCACCGTTCCA	152	60	NM_001101683.1

Assessing the purity of the LCM specimens: To confirm the specificity and purity of each LCM cDNA sample extracted from the LCM fragments combined from a single cornea, all samples were screened for epithelial and stromal cell markers with real-time PCR. Keratin 3 (K3) and Keratin 12 (K12) were used as the epithelium markers [31], and keratocan was used as the keratocyte marker [32]. The primers used for the analyses are listed in Table 1. Expression of keratocan was detected in all anterior stromal cDNAs prepared using LCM (Figure 3). The epithelial markers were not detected in any of the AS LCM cDNA samples. This result confirmed that each AS specimen was free of epithelial contamination.

Analysis of corneal EBM components at different time points after PRK: The expression of key lamina lucida and lamina densa component mRNAs of nidogen-1, nidogen-2, perlecan, and LAMA3 were analyzed with quantitative real-time PCR at 2, 4, and 7 days post −4.5D and −9.0D PRK. These time points were selected based on the results of preliminary TEM studies in which the lamina lucida and lamina densa layers of the EBM were found to fully regenerate in the −4.5D PRK corneas (Table 2) but not the −9.0D PRK corneas [1], at 8 to 10 days after surgery. Thus, the corneas were analyzed during the time interval when cells would be expected to produce components to regenerate the EBM lamina lucida and lamina densa.

Table 2. Rabbit corneas at different time points after −4.5D PRK analyzed with TEM at 23,000X Mag.

Days	n	LL/LD
7	2	- / -
8	2	- / +
9	2	+ / -
10	1	+
11	2	+ / +
13	1	+
15	1	+
17	1	+
19	2	+ / +

+ indicates lamina lucida and lamina densa fully-regenerated in minimum 95% of PRK ablated zone. - indicates lamina lucida and lamina densa detected in less than 95% of the PRK ablated zone.

At 2 days post PRK (Figure 4), the relative levels of nidogen-1 mRNA in the anterior stroma were not statistically significantly different between the −4.5D PRK, −9.0D PRK, and unwounded control corneas. The nidogen-2, perlecan, and LAMA3 mRNAs were statistically significantly higher in the anterior stroma of the −4.5D PRK and −9.0D PRK corneas compared to the unwounded control corneas (Figure 4). The nidogen-2 and laminin α-3 mRNA levels were statistically significantly higher in the −9.0D PRK corneas than in the −4.5D PRK corneas at 2 days after surgery (Figure 4). These results suggest that the anterior stromal cells produce corneal EBM components to facilitate regeneration of the lamina lucida and the lamina densa.

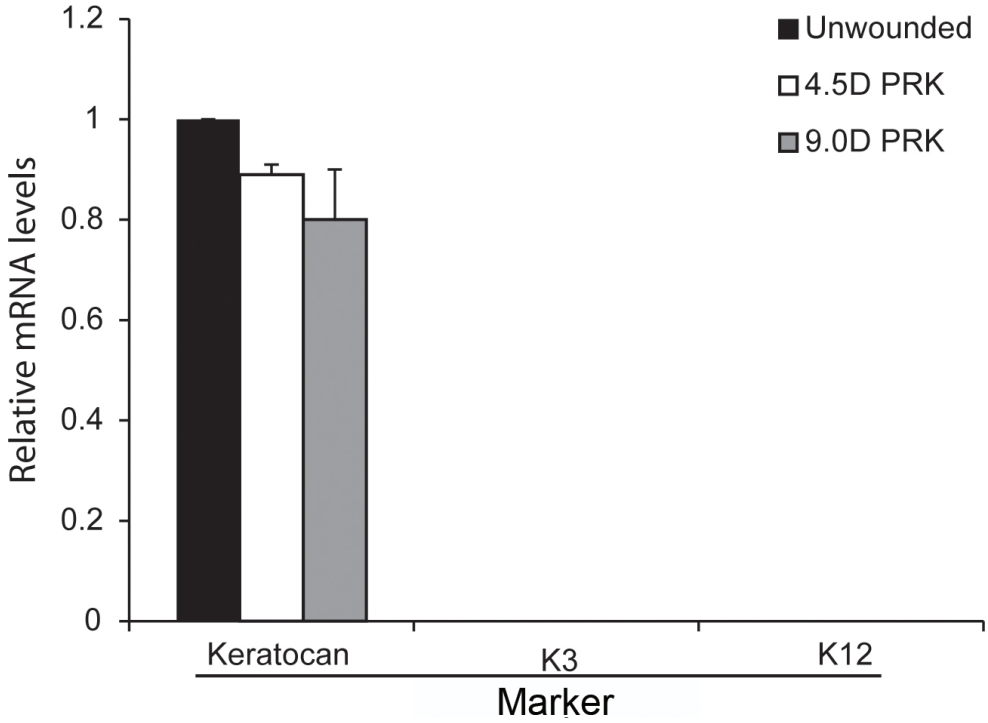

Figure 3. Verification with LCM-RT–PCR of the lack of epithelial contamination in −4.5D PRK, −9.0D PRK, or unwounded control corneas. cDNA of laser capture microdissection (LCM) fragments cut from the anterior stroma of each cornea (as shown in Figure 2) were analyzed using quantitative real-time PCR for keratocan (a keratocyte marker) and keratin 3 (K3) and keratin 12 (K12; epithelial cell markers). Keratocan (keratocytes), but not K3 or K12, mRNA was detected in all three types of anterior stromal samples. Any cDNA sample that showed K3 or K12 contamination was discarded, and cDNA was prepared from newly cut LCM fragments.

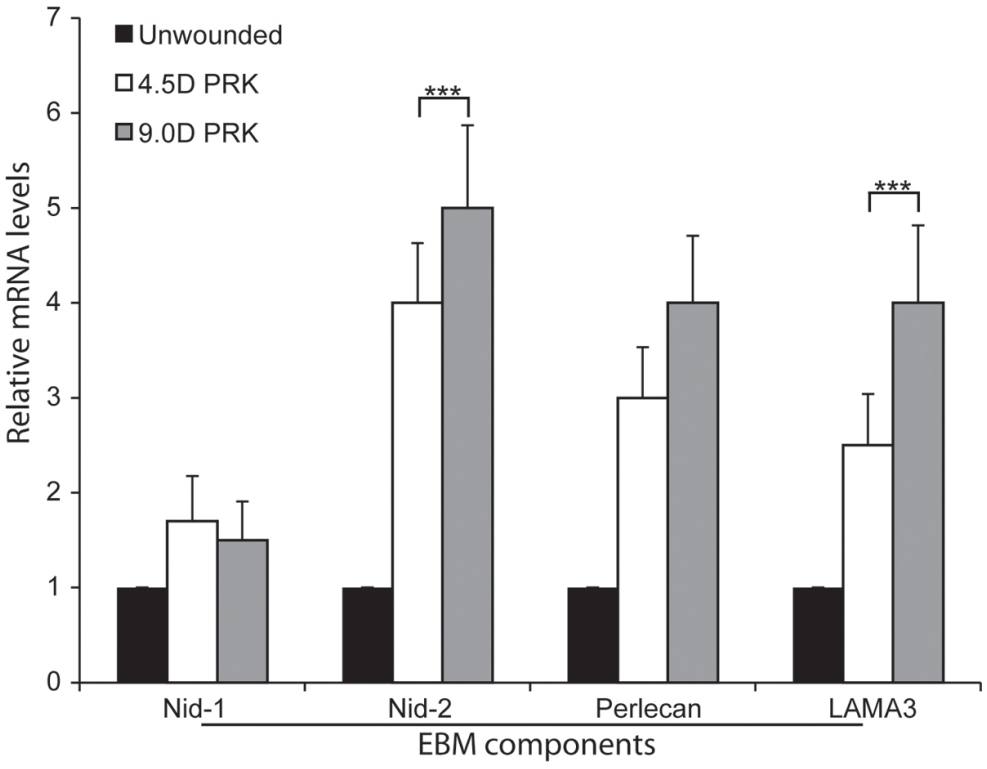

Figure 4. Analysis of EBM component mRNAs in the anterior stroma at 2 days after PRK with quantitative real-time PCR. Nidogen-1 (Nid-1) mRNA was not statistically significantly increased in the anterior stroma of −4.5D photorefractive keratectomy (PRK) or −9.0D PRK corneas compared with the unwounded control corneas at this early time point. The nidogen-2 (Nid-2), perlecan, and laminin α-3 (LAMA3) mRNAs were statistically significantly increased in the anterior stroma of the −4.5D PRK and −9.0D PRK corneas compared to the unwounded control corneas. The Nid-2 and LAMA3 mRNAs were statistically significantly increased in the anterior stroma at 2 days after surgery in the −9.0D PRK corneas compared with the −4.5D PRK corneas. (n = 4 for each group; ***, p<0.01; **`).

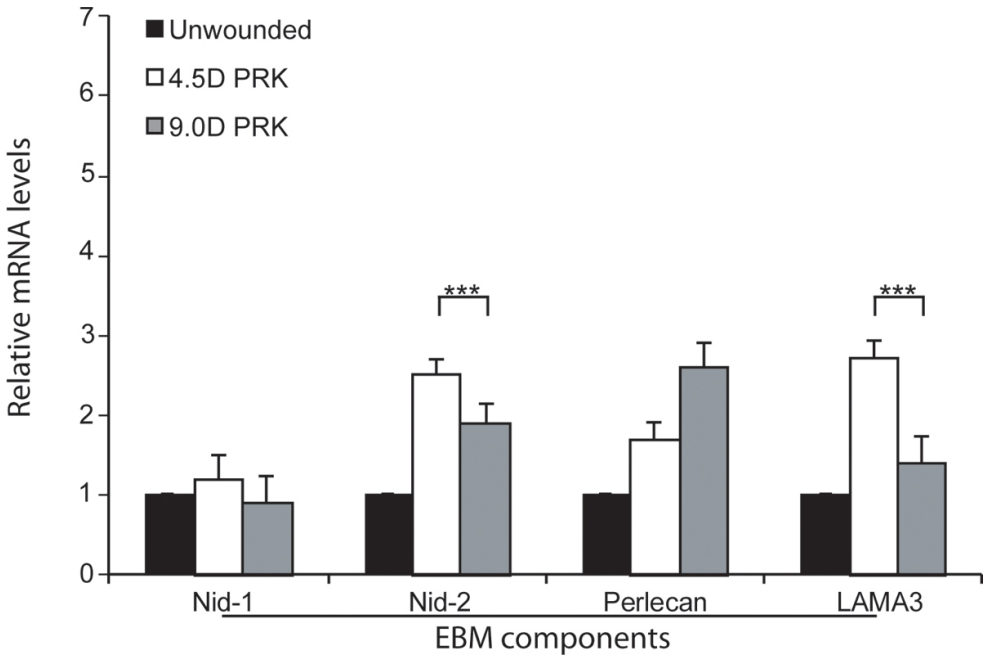

Figure 5. Analysis of EBM component mRNAs in the anterior stroma at 4 days after PRK with quantitative real-time PCR. Nidogen-1 (Nid-1) mRNA was not statistically significantly different in the −4.5D photorefractive keratectomy (PRK), −9.0D PRK, or unwounded control corneas. The nidogen 2 (Nid-2), perlecan, and laminin α-3 (LAMA3) mRNAs were statistically significantly higher in the anterior stroma of the −4.5D PRK and −9.0D PRK corneas compared to the unwounded control corneas. The nidogen-2 and laminin α-3 mRNA levels were statistically significantly higher in the anterior stroma of the −4.5D PRK corneas destined to maintain transparency and regenerate the epithelial basement membrane (EBM) than in the −9.0D PRK corneas destined to develop stromal opacity and not regenerate the EBM at 4 days after surgery. (n = 4 for each group; ***, p<0.01).

At 4 days post-PRK (Figure 5), the relative nidogen-1 mRNA levels were not statistically significantly different in the anterior stroma of the −4.5D PRK, −9.0D PRK, and non-wounded control corneas. The nidogen-2 and perlecan mRNAs in the anterior stromal were statistically significantly higher in the −4.5D and −9.0D PRK corneas than in the unwounded control corneas (Figure 5), and the nidogen-2 mRNAs were statistically significantly higher in the −4.5D PRK corneas destined to regenerate the EBM than in the −9.0D PRK corneas destined to not regenerate the EBM and develop dense fibrosis. The laminin α-3 mRNAs were statistically significantly upregulated in the anterior stroma of the −4.5D PRK corneas, but the mRNA levels were not statistically significantly different between the −9.0D PRK and unwounded control corneas (Figure 5).

At 7 days post-PRK (Figure 6), the nidogen-1 and laminin α-3 mRNA levels were statistically significantly higher in the anterior stroma of the −4.5D PRK and −9.0D PRK corneas than in the unwounded control corneas, and the laminin α-3 mRNA levels were statistically significantly higher in the anterior stroma of the −4.5D PRK corneas than in the −9.0D PRK corneas (Figure 6). The nidogen-2 mRNA levels in the anterior stroma were statistically significantly higher in the −4.5D PRK corneas than in the −9.0D PRK or unwounded control corneas (Figure 6). The perlecan mRNA levels were not statistically significantly different in the anterior stroma of the three groups (Figure 6). All mRNA-level experiments were repeated at least once for each PRK and unwounded control group at each time point, and the results were consistent between the different experiments.

LCM-RT–PCR was also performed on pure full-thickness LCM epithelial specimens of control unwounded, −4.5D PRK, and −9.0D PRK corneas at 5 days after surgery. In the unwounded control corneas, and at time points after wounding when the epithelial defects had fully closed in the −4.5D PRK and −9.0D PRK corneas (approximately 4 days after injury), the laminin α-3, perlecan, nidogen-1, and nidogen-2 mRNAs were also expressed in the corneal epithelium (not shown).

DISCUSSION

Transmission electron microscopy studies have demonstrated that ultrastructural abnormalities in the regeneration of the corneal EBM, including the absence of the lamina lucida and the lamina densa, play a role in the development of myofibroblasts and fibrosis (haze) after major injuries to the epithelium and the stroma, such as high-correction PRK without mitomycin C [1-4] or bacterial corneal ulcers (G. Marino and S.E. Wilson, unpublished data, 2016). These structural defects in the EBM likely correlate with functional EBM defects that allow epithelium-derived TGFβ and PDGF to penetrate into the anterior stroma at sustained levels necessary to drive the

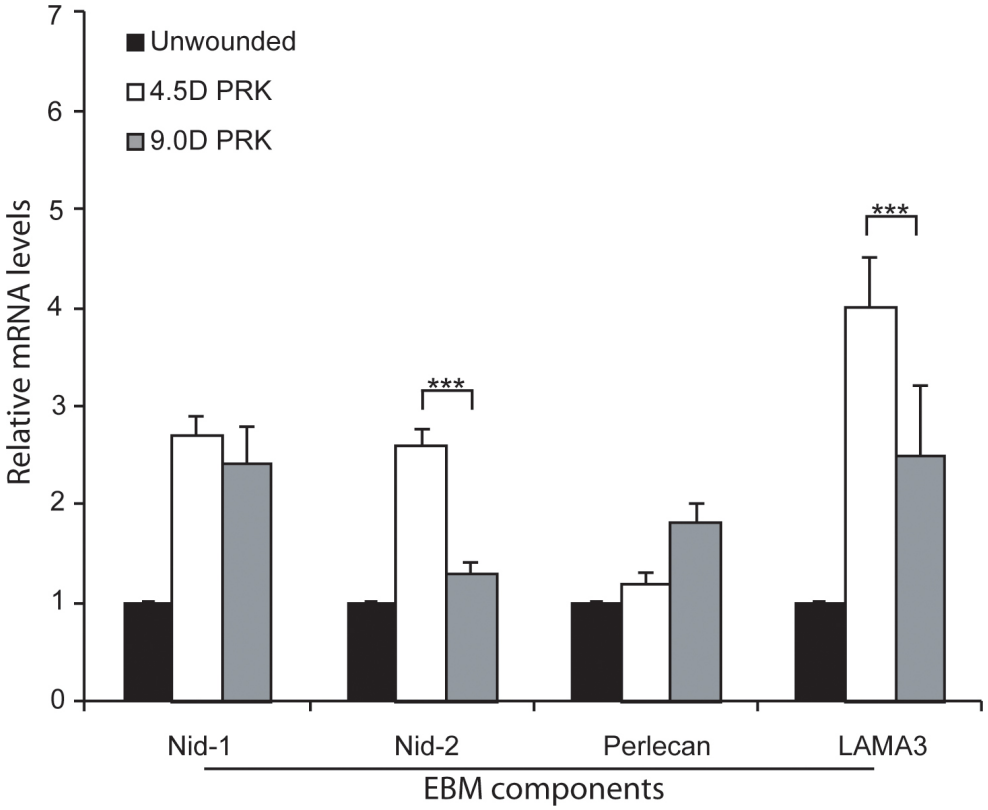

Figure 6. Analysis of EBM component mRNAs in the anterior stroma at 7 days after PRK with quantitative real-time PCR. Nidogen-1 mRNA was statistically significantly increased in the anterior stroma of the −4.5D photorefractive keratectomy (PRK) and −9.0D PRK corneas compared to the unwounded control corneas, but the PRK groups were not statistically significantly different from each other. The nidogen-2 mRNA was statistically significantly higher in the anterior stroma of the −4.5D PRK corneas at this time point just before ultrastructural epithelial basement membrane (EBM) regeneration compared to the −9.0D PRK corneas that are destined to not have ultrastructural EBM regeneration, and only the −4.5D PRK group was statistically significantly higher than the unwounded control group. LAMA3 mRNA was statistically significantly increased in the anterior stroma of the −4.5D PRK corneas at 7 days after surgery compared to the −9.0D PRK corneas or the unwounded control corneas. The difference between the −9.0D PRK corneas and the unwounded control corneas for LAMA3 did not reach statistical significance. The perlecan mRNAs were not statistically significantly increased in the anterior stroma of the PRK corneas from either group or the unwounded control corneas group. (n = 4 for each group; ***, p<0.01).

development of myofibroblast cells from keratocyte- and bone marrow–derived precursor cells (Figure 1D) [1-4,7,8].

One of the most intriguing aspects of haze formation is that it rarely occurs in rabbit or human eyes that have minor injuries such as PRK for lower levels of myopia—even without mitomycin C treatment—although the procedure is otherwise identical to PRK for higher levels of myopia without mitomycin C. Thus, human or rabbit eyes that have PRK for less than −6.0D of myopia rarely develop significant haze [33-35]. As the level of correction increases beyond −6.0D, however, the incidence of haze and the density of the myofibroblasts in the anterior stroma increase in 2–5% of human corneas and in 100% of rabbit corneas [33-35]. Stromal surface irregularity caused by surgery, infection, or injury can mechanically impede EBM regeneration and result in anterior stromal fibrosis or haze [36]. The present study, however, supports the hypothesis that decreased production of EBM components laminin α-3 and nidogen-2 by cells in the anterior stroma at relatively early time points from 4 to 7 days after injury, and before the EBM fully regenerates, is a factor in defective EBM regeneration after more severe injuries (−9.0D PRK, for example) compared to less severe injuries (−4.5D PRK, for example) and leads to myofibroblast development and persistence, and associated anterior stromal fibrosis (haze). Although we have examined stromal cell production of mRNAs coding for laminin α-3, nidogen-1, nidogen-2, and perlecan that are known components of the lamina lucida and the lamina densa, other basement membrane components (including other laminins and collagens) we have not studied could also be produced by keratocytes and deficiencies of these other components could contribute to defective EBM regeneration after corneal injury, infection, or surgery. These fibrotic mechanisms likely also apply to non-healing epithelial defects after corneal injury, infection, or surgery. In situations where the epithelium does not close within 1 to 2 weeks, clearly even the nascent EBM is not laid down over the bare stroma, and TGFβ/PDGF from the peripheral epithelium and/or the tear film penetrates the stroma and drives the development of mature myofibroblasts from precursor cells.

A limitation of this study is the inability to monitor the expression of laminin α-3, nidogen-1, nidogen-2, or perlecan

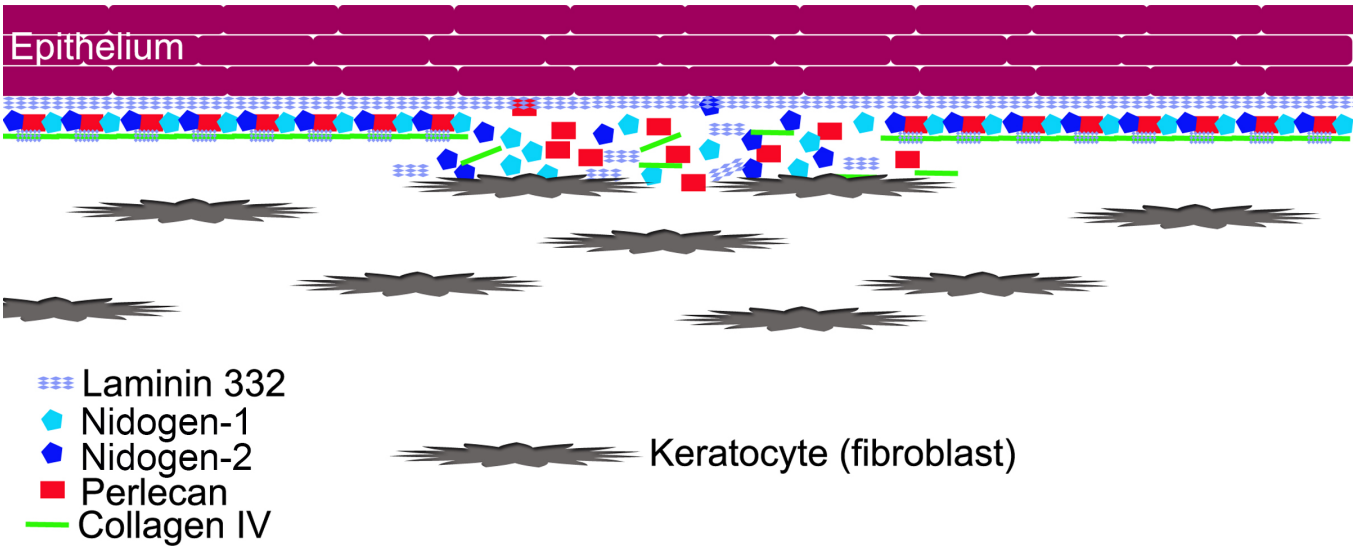

Figure 7. Schematic diagram illustrating hypothesized keratocyte contributions to EBM regeneration. We hypothesize that after corneal epithelial and epithelial basement membrane (EBM) injury, the epithelial defect heals, and the epithelium lays down self-polymerizing laminin 332 to form a nascent EBM. Once this layer is laid down, it forms a barrier that limits to some extent posterior penetration of the other EBM components needed to produce the structurally and functionally mature more posterior basement membrane that includes the lamina lucida and the lamina densa. These components must be provided by contiguous keratocytes that possibly need to be in direct contact with the nascent EBM based on the morphology and ultrastructure noted with TEM in Figure 1A–C. These components provided by keratocytes could include laminin chains (such as laminin α-3), nidogens, perlecan, collagens (such as collagen type IV), and other components. In the rabbit PRK model, the laminin α-3 and nidogen-2 mRNAs were decreased in the anterior stroma of the corneas that had −9.0D photorefractive keratectomy (PRK) compared to the corneas that had −4.5D PRK during the days just before the appearance of the normal regenerated EBM in the corneas that do not develop fibrosis.

proteins in rabbit corneas. Multiple antibodies to the corresponding human and mouse proteins, including those that worked for immunocytochemistry for cultured rabbit cells in vitro [11], were tested but were not useful to localize proteins in rabbit tissues. However, studies detected upregulation of perlecan and nidogen-2 proteins in the keratocytes of human corneas within minutes of epithelial scrape injury [10]; therefore, it is likely the proteins are also expressed in rabbit corneal stromal cells and have altered expression after corneal injury. Connective tissue or mesenchymal tissue cells have been shown to produce basement membrane components in many other organs [12-19].

As the level of epithelial-stromal injury to corneas increases, the number and stromal depth of keratocytes undergoing apoptosis increase [35]. This keratocyte and anterior stromal apoptosis response (including bone marrow–derived cells invading the cornea) continues for a week or more after the injury [35]. Our working hypothesis is that once the healing corneal epithelium lays down the initial self-polymerizing laminin layer of the nascent EBM [26], deeper EBM components, including those that comprise the lamina lucida and the lamina densa, must, at least partially, be contributed by stromal cells (Figure 7). In in vitro studies, nidogen-1 and nidogen-2 mRNAs were highly expressed in keratocytes, and perlecan was highly expressed in myofibroblasts, whereas corneal fibroblasts produced only small quantities of all three of these EBM components [11]. However, intracellular localization of the EBM components was also different between keratocytes and myofibroblasts. In keratocytes, nidogen-2 and perlecan proteins were noted predominantly in intracellular organelles, whereas in myofibroblasts both EBM component proteins were spread diffusely throughout the cell. Thus, we hypothesize that myofibroblasts cannot function to localize EBM components to the nascent EBM that forms after injury as do keratocytes.

Immediately after epithelial or epithelial-stromal injury-induced anterior keratocyte apoptosis [35], bone marrow–derived cells invade the stroma in large numbers [7]. In every injured cornea, a race of sorts occurs between keratocyte repopulation of the anterior stroma and restoration of the normal EBM structure and function versus the development of myofibroblast precursors into mature myofibroblasts that will produce stromal fibrosis. If the injury is not severe (for example, epithelial scrape or low-correction PRK), keratocytes quickly repopulate the anterior stroma, the EBM is restored, and the developing myofibroblasts

undergo apoptosis when they are deprived of high levels of epithelial TGFβ and PDGF needed for survival [8,36]. If the epithelial-stromal injury is severe (for example, −9.0D PRK or severe stromal keratitis) or a rough stromal surface mechanically impedes EBM regeneration [37], then the keratocyte repopulation of the anterior stroma is delayed, or their function is impeded, and myofibroblast precursors (bone marrow–derived and keratocyte-corneal fibroblast-derived [7,8]) become established in the anterior stroma and develop into mature vimentin+, alpha-smooth muscle actin+, and desmin+ (V+A+D+) myofibroblasts (Figure 1D and Figure 2) [6,35]. In the latter case, normal EBM structure and function is not restored, persistently high levels epithelium-derived TGFβ and PDGF penetrate into the stroma, myofibroblasts (themselves opaque [38]) produce large amounts of disordered extracellular matrix (Figure 1D), and fibrosis (haze) develops in the cornea.

Species variation in this process of fibrosis generation is especially interesting. Thus, in rabbits, 100% of corneas that have −9.0D PRK injury show defective EBM regeneration, mature myofibroblast repopulation of the anterior stroma, and accumulation of the disordered extracellular matrix associated with fibrosis and loss of transparency. In humans, however, only 2% to 5% of corneas that have high-correction PRK without mitomycin C develop mature myofibroblasts and fibrosis [21,22]. The majority of these high-correction PRK corneas in humans have the anterior stroma repopulated by keratocytes with few, if any, mature myofibroblasts developing and little disordered extracellular matrix deposited. Teleologically thinking, myofibroblast precursors and mature myofibroblasts have vested interests in impeding EBM regeneration lest the levels of TGFβ and PDGF that penetrate from the epithelium in the absence of normal EBM barrier function decline and these cells undergo apoptosis. They accomplish this by establishing stacked layers of myofibroblasts beneath the epithelium (Figure 1D) that physically impede repopulation of the anterior stroma with keratocytes.

Eventually, even the most fibrotic corneas can clear fibrosis and regain at least some level of transparency [39,40]. In the rabbit model, severe anterior stromal fibrosis typically clears within months [3,4]. Clearing occurs in a spotty distribution across the cornea with the appearance of clear lacunas where the EBM has finally regenerated, myofibroblasts have undergone apoptosis, and keratocytes have repopulated the subepithelial stroma—where they reabsorb the disordered extracellular matrix and reestablish the normal extracellular matrix associated with corneal transparency. These lacunas expand and coalesce over time until complete corneal transparency can be restored. This process takes approximately 3 to 4 months after −9.0D PRK injury in rabbits (G. Marino and S.E. Wilson, unpublished data, 2016). Similar restoration of transparency in human corneas that develop anterior stromal fibrosis after high-correction PRK typically takes years [21,22]. Some human corneas do not have a return of transparency even many years following severe injuries or infections. Presumably, in these cases the fibrosis remains because the EBM is never regenerated, and the mature myofibroblasts and the disordered extracellular matrix they produce persist in the affected stroma. It is possible that measures to augment the production or delivery of EBM components by corneal stromal cells or to facilitate anterior stromal repopulation by keratocytes could be effective therapeutic measures to decrease corneal fibrosis or haze after corneal injury, infection, and surgery.

Fibrosis is common to the pathophysiology of diseases in many organs, including primary idiopathic pulmonary fibrosis in the lung [41-43], hypertrophic scars in the skin [44,45], fibrosis of the heart [46] and fibrosis of the kidney [47-49]. We hypothesize that the model of epithelial-EBM injury and defective EBM regeneration associated with fibrosis in the cornea is relevant to other organs where there is chronic injury to parenchymal cells or defective basement membranes or imperfect regeneration of basement membranes.

ACKNOWLEDGMENTS

Supported in part by US Public Health Service grants EY10056 and EY015638 from the National Eye Institute, National Institutes of Health, Bethesda, MD and Research to Prevent Blindness, New York, NY.

REFERENCES

1. Torricelli AA, Singh V, Agrawal V, Santhiago MR, Wilson SE. Transmission electron microscopy analysis of epithelial basement membrane repair in rabbit corneas with haze. Invest Ophthalmol Vis Sci 2013; 54:4026-33. [PMID: 23696606].
2. Torricelli AA, Singh V, Santhiago MR, Wilson SE. The corneal epithelial basement membrane: structure, function, and disease. Invest Ophthalmol Vis Sci 2013; 54:6390-400. [PMID: 24078382].
3. Torricelli AAM, Wilson SE. Cellular and extracellular matrix modulation of corneal stromal opacity. Exp Eye Res 2014; 129:151-60. [PMID: 25281830].
4. Torricelli AAM, Santhanam A, Wu J, Singh V, Wilson SE. The corneal fibrosis response to epithelial-stromal injury. Exp Eye Res 2016; 142:110-8. [PMID: 26675407].
5. Jester JV, Petroll WM, Cavanagh HD. Corneal stromal wound healing in refractive surgery: the role of myofibroblasts. Prog Retin Eye Res 1999; 18:311-56. [PMID: 10192516].

6. Chaurasia SS, Kaur H, Medeiros FW, Smith SD, Wilson SE. Dynamics of the expression of intermediate filaments vimentin and desmin during myofibroblast differentiation after corneal injury. Exp Eye Res 2009; 89:133-9. [PMID: 19285070].

7. Barbosa FL, Chaurasia S, Cutler A, Asosingh K, Kaur H, de Medeiros F, Agrawal V, Wilson SE. Corneal myofibroblast generation from bone marrow-derived cells. Exp Eye Res 2010; 91:92-6. [PMID: 20417632].

8. Singh V, Jaini R, Torricelli AA, Santhiago M, Singh N, Ambati BK, Wilson SE. TGFβ and PDGF-B signaling blockade inhibits myofibroblast development from both bone marrow-derived and keratocyte-derived precursor cells in vivo. Exp Eye Res 2014; 121:35-40. [PMID: 24582892].

9. Hassell JR, Schrecengost PK, Rada JA, SundarRaj N, Sossi G, Thoft RA. Biosynthesis of stromal matrix proteoglycans and basement membrane components by human corneal fibroblasts. Invest Ophthalmol Vis Sci 1992; 33:547-57. [PMID: 1544783].

10. Torricelli AAM, Marino GK, Santhanam A, Wu J, Singh A, Wilson SE. Epithelial basement membrane proteins perlecan and nidogen-2 are up-regulated in stromal cells after epithelial injury in human corneas. Exp Eye Res 2015; 134:33-8. [PMID: 25797478].

11. Santhanam A, Torricelli AAM. Wu, Marino GK, Wilson SE. Differential expression of epithelial basement membrane components nidogens-1 and −2 and perlecan in corneal stromal cells in vitro. Mol Vis 2015; 21:1318-27. [PMID: 26788024].

12. Marinkovich MP, Keene DR, Rimberg CS, Burgeson RE. Cellular origin of the dermal-epidermal basement membrane. Dev Dyn 1993; 197:255-67. [PMID: 8292823].

13. Fox JW, Mayer U, Nischt R, Aumailley M, Reinhardt D, Wiedemann H, Mann K, Timpl R, Krieg T, Engel J, Chu ML. Recombinant nidogen consists of three globular domains and mediates binding of laminin to collagen type IV. EMBO J 1991; 10:3137-46. [PMID: 1717261].

14. El Ghalbzouri A, Jonkman MF, Dijkman R, Ponec M. Basement membrane reconstruction in human skin equivalents is regulated by fibroblasts and/or exogenously activated keratinocytes. J Invest Dermatol 2005; 124:79-86. [PMID: 15654956].

15. Simon-Assmann P, Bouziges F, Arnold C, Haffen K, Kedinger M. Epithelial-mesenchymal interactions in the production of basement membrane components in the gut. Development 1988; 102:339-47. [PMID: 17061377].

16. Fleischmajer R, Utani A, MacDonald ED, Perlish JS, Pan TC, Chu ML, Nomizu M, Ninomiya Y, Yamada Y. Initiation of skin basement membrane formation at the epidermo-dermal interface involves assembly of laminins through binding to cell membrane receptors. J Cell Sci 1998; 111:1929-40. [PMID: 9645941].

17. El Ghalbzouri A, Ponec M. Diffusible factors released by fibroblasts support epidermal morphogenesis and deposition of basement membrane components. Wound Repair Regen 2004; 12:359-67. [PMID: 15225215].

18. Smola H, Stark HJ, Thiekötter G, Mirancea N, Krieg T, Fusenig NE. Dynamics of basement membrane formation by keratinocyte-fibroblast interactions in organotypic skin culture. Exp Cell Res 1998; 239:399-410. [PMID: 9521858].

19. Furuyama A, Kimata K, Mochitate K. Assembly of basement membrane in vitro by cooperation between alveolar epithelial cells and pulmonary fibroblasts. Cell Struct Funct 1997; 22:603-14. [PMID: 9591052].

20. Miosge N. The ultrastructural composition of basement membranes in vivo. Histol Histopathol 2001; 16:1239-48. [PMID: 11642743].

21. Hersh PS, Stulting RD, Steinert RF, Waring GO 3rd, Thompson KP, O'Connell M, Doney K, Schein OD. Results of phase III excimer laser photorefractive keratectomy for myopia. The Summit PRK Study Group. Ophthalmology 1997; 104:1535-53. [PMID: 9331190].

22. Rajan MS, Jaycock P, O'Brart D, Nystrom HH, Marshall J. A long-term study of photorefractive keratectomy; 12-year follow-up. Ophthalmology 2004; 111:1813-24. [PMID: 15465541].

23. Kabosova A, Azar DT, Bannikov GA, Campbell KP, Durbeej M, Ghohestani RF, Jones JC, Kenney MC, Koch M, Ninomiya Y, Patton BL, Paulsson M, Sado Y, Sage EH, Sasaki T, Sorokin LM, Steiner-Champliaud MF, Sun TT, Sundarraj N, Timpl R, Virtanen I, Ljubimov AV. Compositional differences between infant and adult human corneal basement membranes. Invest Ophthalmol Vis Sci 2007; 48:4989-99. [PMID: 17962449].

24. Kruegel J, Miosge N. Basement membrane components are key players in specialized extracellular matrices. Cell Mol Life Sci 2010; 67:2879-95. [PMID: 20428923].

25. Tuori A, Uusitalo H, Burgeson RE, Terttunen J, Virtanen I. The immunohistochemical composition of the human corneal basement membrane. Cornea 1996; 15:286-94. [PMID: 8713932].

26. Yurchenco PD. Basement membranes: cell scaffoldings and signaling platforms. Cold Spring Harb Perspect Biol 2011; 3:a0049111-27. [PMID: 21421915].

27. Bonner RF, Emmert-Buck M, Cole K, Pohida T, Chuaqui R, Goldstein S, Liotta LA. Laser capture microdissection: molecular analysis of tissue. Science 1997; 278:1481-3. [PMID: 9411767].

28. Emmert-Buck MR, Bonner RF, Smith PD, Chuaqui RF, Zhuang Z, Goldstein SR, Weiss RA, Liotta LA. Laser capture microdissection. Science 1996; 274:998-1001. [PMID: 8875945].

29. Fantes FE, Hanna KD, Waring GO 3rd, Pouliquen Y, Thompson KP, Savoldelli M. Wound healing after excimer laser keratomileusis (photorefractive keratectomy) in monkeys. Arch Ophthalmol 1990; 108:665-75. [PMID: 2334323].

30. Arocho A, Chen B, Ladanyi M, Pan Q. Validation of the 2-DeltaDeltaCt calculation as an alternate method of data analysis for quantitative PCR of BCR-ABL P210 transcripts. Diagn Mol Pathol 2006; 15:56-61. [PMID: 16531770].

31. Liu JJ, Kao WW, Wilson SE. Corneal epithelium-specific mouse keratin K12 promoter. Exp Eye Res 1999; 68:295-301. [PMID: 10079137].

32. Funderburgh JL, Mann MM, Funderburgh ML. Keratocyte phenotype mediates proteoglycan structure: a role for fibroblasts in corneal fibrosis. J Biol Chem 2003; 278:45629-37. [PMID: 12933807].

33. Hersh PS, Stulting RD, Steinert RF, Waring GO 3rd, Thompson KP, O'Connell M, Doney K, Schein OD. Results of phase III excimer laser photorefractive keratectomy for myopia. The Summit PRK Study Group. Ophthalmology 1997; 104:1535-53. [PMID: 9331190].

34. Siganos DS, Katsanevaki VJ, Pallikaris IG. Correlation of subepithelial haze and refractive regression 1 month after photorefractive keratectomy for myopia. J. Ref. Surg. 1999; 15:338-42. [PMID: 10367577].

35. Mohan RR, Hutcheon AEK, Choi R, Hong J-W, Lee J-S, Mohan RR, Ambrósio R, Zieske JD, Wilson SE. Apoptosis, necrosis, proliferation, and myofibroblast generation in the stroma following LASIK and PRK. Exp Eye Res 2003; 76:71-87. [PMID: 12589777].

36. Jester JV, Barry-Lane PA, Petroll WM, Olsen DR, Cavanagh HD. Inhibition of corneal fibrosis by topical application of blocking antibodies to TGF beta in the rabbit. Cornea 1997; 16:177-87. [PMID: 9071531].

37. Netto MV, Mohan RR, Sinha S, Sharma A, Dupps W, Wilson SE. Stromal haze, myofibroblasts, and surface irregularity after PRK. Exp Eye Res 2006; 82:788-97. [PMID: 16303127].

38. Jester JV, Moller-Pedersen T, Huang J, Sax CM, Kays WT, Cavangh HD, Petroll WM, Piatigorsky J. The cellular basis of corneal transparency: evidence for 'corneal crystallins'. J Cell Sci 1999; 112:613-22. [PMID: 9973596].

39. Hassell JR, Cintron C, Kublin C, Newsome DA. Proteoglycan changes during restoration of transparency in corneal scars. Arch Biochem Biophys 1983; 222:362-9. [PMID: 6847191].

40. Rawe IM, Meek KM, Leonard DW, Takahashi T, Cintron C. Structure of corneal scar tissue: an X-ray diffraction study. Biophys J 1994; 67:1743-8. [PMID: 7819506].

41. Strieter RM. What differentiates normal lung repair and fibrosis? Inflammation, resolution of repair, and fibrosis. Proc Am Thorac Soc 2008; 5:305-10. [PMID: 18403324].

42. Coward WR, Saini G, Jenkins G. The pathogenesis of idiopathic pulmonary fibrosis. The Adv Rspir Dis. 2010; 4:367-88. [PMID: 20952439].

43. Strieter RM, Mehrad B. New mechanisms of pulmonary fibrosis. Chest 2009; 136:1364-70. [PMID: 19892675].

44. Hellström M, Hellström S, Engström-Laurent A, Bertheim U. The structure of the basement membrane zone differs between keloids, hypertrophic scars and normal skin: a possible background to an impaired function. J Plast Reconstr Aesthet Surg 2014; 67:1564-72. [PMID: 25037500].

45. Yang L, Hashimoto K, Shirakata Y. Epidermogenesis in a skin wound deep through the basement membrane contributes to scar formation. J Dermatol Sci 2012; 65:224-6. [PMID: 22300814].

46. Kanisicak O, Khalil H, Ivey MJ, Karch J, Maliken BD, Correll RN, Brody MJ, Lin S-CJ, Aronow BJ, Tallquist MD, Molkentin JD. Genetic lineage tracing defines myofibroblast origin and function in the injured heart. Nat Commun 2016; 7:12260-[PMID: 27447449].

47. Sun YBY, Qu X, Caruana G, Li J. The origin of renal fibroblasts/myofibroblasts and the signals that trigger fibrosis. Differentiation 2016; [PMID: 27262400].

48. Humphreys BD, Lin S-L, Kobayashi A, Hudson TE, Nowlin BT, Bonventre JV, Valerius MT, McMahon AP, Duffield JS. Fate Tracing Reveals the Pericyte and Not Epithelial. 1. Origin of Myofibroblasts in Kidney Fibrosis. Am J Pathol 2010; 176:85-97. [PMID: 20008127].

49. Mack M, Yanagita M. Origin of myofibroblasts and cellular events triggering fibrosis. Kidney Int 2015; 87:297-307. [PMID: 25162398].

Articles are provided courtesy of Emory University and the Zhongshan Ophthalmic Center, Sun Yat-sen University, P.R. China. The print version of this article was created on 26 February 2017. This reflects all typographical corrections and errata to the article through that date. Details of any changes may be found in the online version of the article.